

Accelerated Intestinal Epithelial Cell Turnover: A New Mechanism of Parasite Expulsion

Laura J. Cliffe,¹ Neil E Humphreys,¹ Thomas E. Lane,²
Chris S. Potten,³ Cath Booth,³ Richard K. Grencis^{1*}

The functional integrity of the intestinal epithelial barrier forms a major defense against invading pathogens, including gastrointestinal-dwelling nematodes, which are ubiquitous in their distribution worldwide. Here, we show that an increase in the rate of epithelial cell turnover in the large intestine acts like an "epithelial escalator" to expel *Trichuris* and that the rate of epithelial cell movement is under immune control by the cytokine interleukin-13 and the chemokine CXCL10. This host protective mechanism against intestinal pathogens has implications for our wider understanding of the multifunctional role played by intestinal epithelium in mucosal defense.

Worm infections are among the most prevalent of all known diseases (1). *Trichuris trichuria*, a cecal-dwelling parasitic nematode, actively penetrates the intestinal epithelium, forming syncytial tunnels through which they move and feed. The intestinal epithelium is under continual renewal. Enterocytes migrate luminally, undergoing proliferation, differentiation, and maturation

before undergoing programmed cell death and extrusion into the intestinal lumen (epithelial cell turnover) (2). The mechanisms through which turnover is controlled remain elusive.

After infection with *T. muris*, the murine model for human whipworm, mouse strains that generate a T helper 2 (TH2) immune response expel their parasites; conversely, mice that generate a TH1 immune response are highly susceptible and maintain infection to chronicity. Interleukin-13 (IL-13) plays a critical role in parasite expulsion (3, 4), and interferon- γ (IFN- γ) is essential for progression to chronic infection (5). The actual effector mechanisms by which parasites are expelled from the intestine remain to be defined, however. Antibody, eosinophils, natu-

ral killer cells, $\gamma\delta$ T cells, and mast cells are not essential (6–8).

We now ask if an elevation in the rate of intestinal epithelial cell turnover acts as an epithelial escalator to displace worms from their optimal niche within the intestine, causing their eventual expulsion by rapidly removing them together with their immediate habitat, the intestinal epithelium. In addition, we assessed whether the increase in rate of turnover was under immune control.

Initially, the levels of epithelial cell proliferation within the cecum were assessed in mice susceptible to infection (AKR) and mice resistant to infection (BALB/c). AKR mice maintained infection to patency, whereas in the BALB/c, expulsion was under way at day 14 and complete by day 21 after infection. In the BALB/c strain, we observed a transient increase in the percentage of cecal epithelial cells undergoing proliferation, with levels returning to baseline following expulsion. However, with the persistence of worms in AKR mice, an elevation in proliferation was evident (Fig. 1, A and B), coincident with the development of crypt-cell hyperplasia throughout the cecum (9) (fig. S1).

In a bromodeoxyuridine (BrdU) pulse-chase experiment (10), the rate of cell turnover was elevated in both strains of mouse after infection, although the increase was almost double in the resistant strain at day 14, the time of worm expulsion (Fig. 1, C and D), when compared with the susceptible AKR strain. Indeed, in the BALB/c mouse, a greater loss of cells from the proliferative compartment (Fig. 1F, positions 0 to 10) and a large net gain of labeled cells higher up the crypt axis clearly illustrated that cells

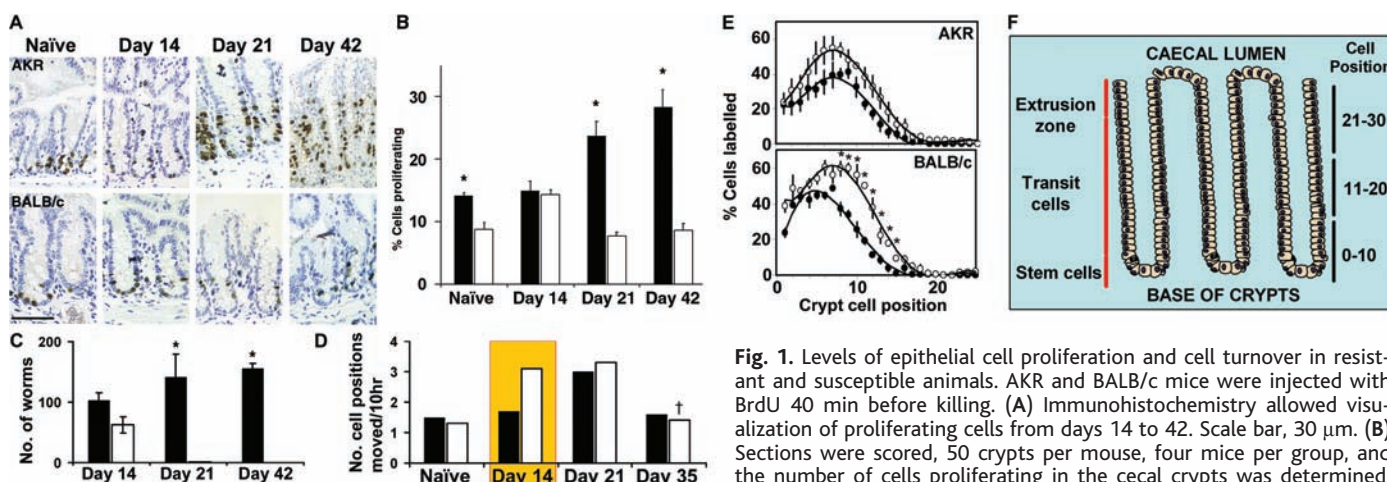


Fig. 1. Levels of epithelial cell proliferation and cell turnover in resistant and susceptible animals. AKR and BALB/c mice were injected with BrdU 40 min before killing. (A) Immunohistochemistry allowed visualization of proliferating cells from days 14 to 42. Scale bar, 30 μ m. (B) Sections were scored, 50 crypts per mouse, four mice per group, and the number of cells proliferating in the cecal crypts was determined. Black bars, AKR; blank bars, BALB/c. Mean \pm SE. *, $P < 0.01$. (C) Worm burden assessed in AKR (black bars) and BALB/c (blank bars). Mean \pm SE. (D) The rate of epithelial cell turnover was assessed by administering BrdU to mice either 40 min or 12 hours before killing. With a position-based analysis, the rate of movement was expressed as number of cell positions moved per 10 hours. AKR, black bars; BALB/c, blank bars. Day 14 is a critical time for parasite expulsion. †, data point for day 28. (E) Positional distribution of labeled cells in AKR and BALB/c mice day 14, expressed as percentage of cells at each position (0 to 30) that were labeled. Black circles, 40 min; open circles, 12 hours. 50 crypts per animal were scored. *, $P < 0.01$. (F) Schematic diagram of epithelial crypts depicting cell positions and transit regions. Data in all panels are mean \pm SE; four animals per group.

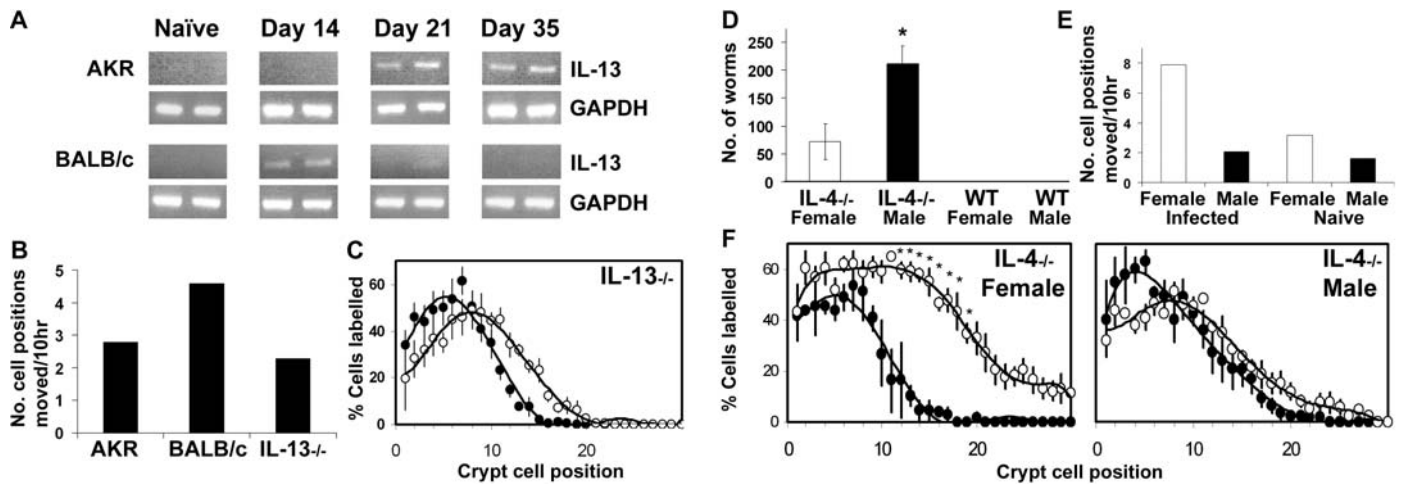


Fig. 2. Importance of IL-13 and GAPDH in epithelial cell turnover. (A) Expression of IL-13 in gut assessed by reverse transcription polymerase chain reaction (RT-PCR) in AKR and BALB/c mice. Each lane represents an individual mouse. (B) The rate of epithelial cell turnover in IL-13^{-/-} mice, day 14. (C) Percentage of labeled cells recorded at each position (0 to 30), day 14 in IL-13^{-/-} animals. Black circles, 40 min; open circles, 12 hours. (D) Worm burden in IL-4^{-/-} female and male animals and

wild-type counterparts, day 28. *, *P* < 0.05. (E) The rate of epithelial cell turnover assessed in male (black bars) and female (blank bars) IL-4^{-/-} mice, both naïve and day 28. (F) Percentage of labeled cells recorded at each cell position (0 to 30) in IL-4^{-/-} female and male mice, day 28. Black circles, 40 min; open circles, 12 hours. *, *P* < 0.01, IL-4^{-/-} female versus male 12-hour BrdU pulse. Data in panels (B) to (F) are mean ± SE; four animals per group.

Table 1. Net change in percentage of labeled cells in each region over 12 hours. The movement of cells up the crypts was determined by calculating the percentage of cells labeled at each position 40 min and 12 hours after the BrdU pulse. By subtracting the values at 40 min from those at 12 hours, the net loss (-) or net gain (+) of cells from one region to the next was ascertained. Day column is days after infection.

Day	Mouse strain and treatment	Net loss (-) or net gain (+) of cells (%)		
		Crypt-cell position		
		0-10	11-20	21-30
14	AKR	+4	+1.50	+0.99
14	BALB/c	-25.80	+24.39	+5.52
14	IL-13 ^{-/-}	-4.16	+3.29	+0.87
28	IL-4 ^{-/-} female	-40.18	+24.78	+15.40
28	IL-4 ^{-/-} male	-14.78	+9.30	+5.48
21	AKR+ control Ig	-26.05	+21.55	+4.50
21	AKR+ mAb to CXCL10	-46.62	+23.95	+21.87
21	SCID+ control Ig	-25.25	+17.25	+8.00
21	SCID+ mAb to CXCL10	-0.48	+13.10	+27.38

were migrating at a much faster rate in resistant animals (Table 1 and Fig. 1E). Moreover, although there was significant crypt hyperplasia in the AKR as infection progressed, this was not seen in BALB/c mice. In fact, a small decrease in crypt size was repeatedly seen on day 14, consistent with an elevation in turnover (fig. S1). In the BALB/c mouse, the parasite is found in the lower/mid region of the crypt at the time the increase in turnover is occurring in this compartment. The elevated rate of turnover seen at day 21 in the AKR strain, to a level comparable to the BALB/c at day 14, suggested that at this later timepoint the level of turnover is not sufficient to displace the parasites, which by now are considerably larger. Between days 14 and 21, *T. muris* will have quadrupled in length and undergone a further molt. They reside much higher in the crypt and are not in the compartment

where the fastest movement of cells is occurring (Table 1 and fig. S2). It is also interesting to note that in both AKR and BALB/c mice, the rate of turnover returned to naïve levels, despite the obvious difference in the presence (AKR) and absence (BALB/c) of worms in the two strains (Fig. 1, C and D). The slow rate of epithelial turnover and high level of proliferation explains the development of crypt-cell hyperplasia associated with chronicity.

IL-13 is a key mediator of gut nematode immunity (3, 4) and is expressed in the intestine of BALB/c mice at the time of worm expulsion (Fig. 2A). IL-13^{-/-} mice and wild-type (BALB/c) mice were infected with 200 *T. muris* eggs, and the rate of turnover was assessed at day 14 (Fig. 2, B and C, and Table 1). It was clear that the rate of turnover in these animals resembled that of a susceptible AKR and not the resistant wild-

type BALB/c, demonstrating a clear role for IL-13.

To assess the relative roles of IL-4 and IL-13 in the response, we examined the capacity of IL-13 to regulate epithelial cell turnover, based on the fact that BALB/c female IL-4^{-/-} mice expel parasites (through an IL-13-dependent mechanism), albeit more slowly than wild-type mice, whereas male IL-4^{-/-} mice suffer chronic infection (4). Both male and female IL-4^{-/-} animals and wild-type animals were infected with *T. muris*, and the rate of turnover was assessed. At day 28, male IL-4^{-/-} animals harbored infection, whereas parasite expulsion was under way in female animals. All wild-type animals had expelled their worms (Fig. 2D). Comparison of the rate of turnover in IL-4^{-/-} mice revealed that female animals had a much faster rate than male animals (Fig. 2E), and significantly greater numbers of labeled cells could be found higher up the crypt axis than in male animals (Fig. 2F and Table 1), again suggesting a prominent role for IL-13 but not IL-4. Interestingly, the rate of cell turnover in female IL-4^{-/-} was twice that seen in BALB/c wild-type mice on day 14 during expulsion (Fig. 1D versus Fig. 2E), again indicating that a greater response is required to expel the larger stages of the parasite.

Chronic *T. muris* infection is dependent on IFN- γ (5), and recently the chemokine CXCL10 [IFN- γ -induced protein 10 (IP-10)] was shown to reduce the rate of epithelial cell turnover in a mouse model of colitis (11). After *T. muris* infection, the expression of CXCL10 was first detected in epithelial cells isolated from the large intestine of susceptible AKR mice at day 21, coincident with the

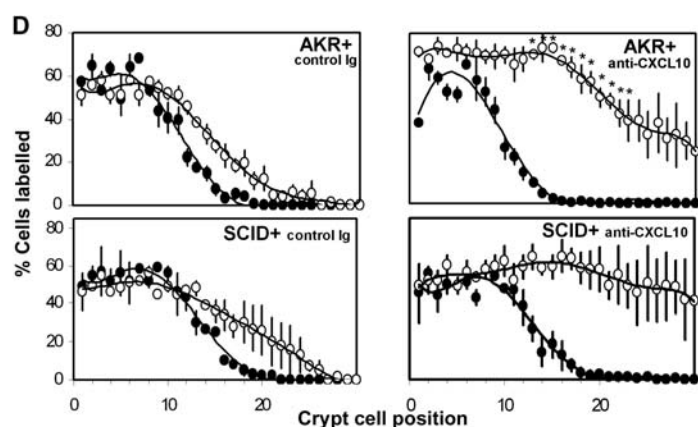
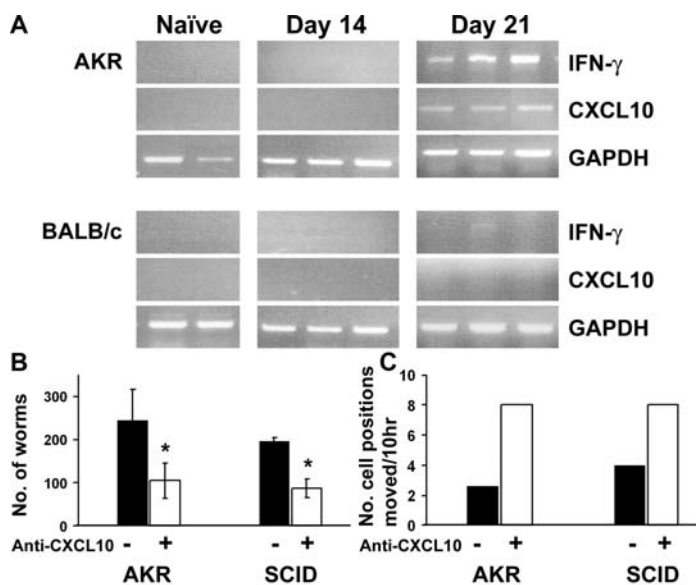


Fig. 3. Manipulation of epithelial cell turnover by neutralizing chemokine CXCL10 causes a significant reduction in worm burden. (A) Expression of CXCL10, IFN- γ , and GAPDH in isolated intestinal epithelium, assessed by RT-PCR in AKR and BALB/c mice infected with *T. muris*. (B) Worm burden assessed in control mAb-treated (black bars) and CXCL10-antibody-treated (blank bars) AKR mice or SCID mice, day 28. *, $P < 0.01$. (C) Rate of epithelial cell turnover assessed on day 21. (D) Percentage of labeled cells recorded at each position (0 to 30) in animals receiving mAb to CXCL10 or control mAb, day 21. Black circles, 40 min; open circles, 12-hour BrdU. *, $P < 0.01$, AKR mice treated versus untreated 12-hour BrdU pulse. Data in all panels are mean \pm SE; four animals per group.

expression of IFN- γ (Fig. 3A and fig. S3A). Both were undetectable in resistant BALB/c mice. The receptor for CXCL10 (CXCR3) was also expressed in the intestine of infected AKR but not BALB/c at the time of CXCL10 induction (fig. S3B). Interestingly, IL-13 was also expressed in the gut of AKR on day 21 and day 35 (Fig. 2A). This would help explain the elevation in turnover seen in AKR on day 21 but also suggests that CXCL10 expression exerts a dominant effect even in the presence of IL-13. In vivo neutralization of CXCL10 in infected AKR mice caused a significant reduction in worm burden by day 28 (Fig. 3B). Furthermore, the treated group of animals showed a highly significant increase in the rate of epithelial cell turnover when compared with untreated animals (Fig. 3C). Also, a much higher proportion of labeled cells could be found higher up the crypt axis in treated animals (Fig. 3D and Table 1). The treatment of these animals with monoclonal antibody (mAb) to CXCL10 had no effect on the ongoing TH1 immune response (figs. S4 and S5) characteristic of a susceptible animal. This strongly suggests that epithelial cell turnover alone can mediate worm expulsion and reinforces the fact that it can remove later stages of the infection if the elevation in turnover is high enough.

Severe combined immunodeficient (SCID) mice lack B cells and T cells and therefore are incapable of generating an adaptive immune response, are highly susceptible to *T. muris* infection, and develop an IFN- γ -driven crypt-cell hyperplasia (9). This provides an ideal situation in which to modulate turnover in the absence of adaptive immunity. SCID mice in which CXCL10 was neu-

tralized showed a significant reduction in worm burden compared with control-treated animals (Fig. 3B). Assessment of the rate of cell turnover clearly illustrated that the in vivo blockade of CXCL10 also significantly elevated the rate of cell turnover in these animals (Fig. 3, C and D, and Table 1). Therefore, elevating the rate of epithelial cell turnover was sufficient to displace parasites from the intestine.

Thus, epithelial cell turnover is an efficient and effective mechanism of gastrointestinal helminth expulsion from the large intestine. Furthermore, the parasite promotes its own survival in susceptible animals by inducing the production of IFN- γ , which acts to drive epithelial cell proliferation (9) and also locally induces CXCL10. This chemokine slows the epithelial escalator, resulting in crypt-cell hyperplasia and an increase in the epithelial niche. Resistant mice counter this in an IL-13-dependent manner, elevating the rate of epithelial cell turnover and displacing the parasite. Recently, a goblet cell-derived factor, RELM β , has been described that is thought to affect the chemosensory apparatus of gastrointestinal-dwelling nematodes, thus impairing their survival (12). RELM β expression is also regulated by IL-13, and the coordinated control of both turnover and RELM β -mediated worm disorientation would be an extremely efficient method of removing the parasites from the gut. This finding identifies immune-mediated control of epithelial homeostasis as being an important mechanism in the control of infectious disease in the intestine. Indeed, many pathogens elicit intestinal hyperplasia under adaptive immune control, for example, *Citrobacter rodentium* (13). Investiga-

tion of epithelial turnover in response to such microbes would give new insights into the array of immune-mediated effector mechanisms that help control infection at mucosal surfaces.

References and Notes

1. A. Montresor, D. W. T. Crompton, T. W. Gyrkos, L. Salvioli, "Helminth control in school-age children: A guide for managers of control programmes" (World Health Organization, Geneva, 2002).
2. C. S. Potten, *Philos. Trans. R. Soc. Lond. B Biol. Sci.* **353**, 821 (1998).
3. A. J. Bancroft, A. N. McKenzie, R. K. Grencis, *J. Immunol.* **160**, 3453 (1998).
4. A. J. Bancroft, D. Artis, D. D. Donaldson, J. P. Sypek, R. K. Grencis, *Eur. J. Immunol.* **30**, 2083 (2000).
5. K. J. Else, F. D. Finkelman, C. R. Maliszewski, R. K. Grencis, *J. Exp. Med.* **179**, 347 (1994).
6. T. D. Lee, D. Wakelin, R. K. Grencis, *Int. J. Parasitol.* **13**, 349 (1983).
7. K. Koyama, *Parasite Immunol.* **24**, 527 (2002).
8. C. J. Betts, K. J. Else, *Parasite Immunol.* **21**, 45 (1999).
9. D. Artis, C. S. Potten, K. J. Else, F. D. Finkelman, R. K. Grencis, *Exp. Parasitol.* **92**, 144 (1999).
10. Materials and methods are available as supporting material on Science Online.
11. S. Sasaki et al., *Eur. J. Immunol.* **32**, 3197 (2002).
12. D. Artis et al., *Proc. Natl. Acad. Sci. U.S.A.* **101**, 13596 (2004).
13. T. T. MacDonald, G. Frankel, G. Dougan, N. S. Gonçalves, C. Simmons, *Int. J. Microbiol.* **293**, 87 (2003).
14. We thank A. N. McKenzie for the IL-13^{-/-} animals, J. Pennock and J. Hankinson for cDNA samples, E. J. Servier for technical assistance, and E. Bell, A. Bancroft, and K. Gull for useful comments and help with the manuscript. This study was supported by the Biotechnology and Biological Sciences Research Council, Epistem Ltd., The Wellcome Trust, and NIH.

Supporting Online Material
www.sciencemag.org/cgi/content/full/308/5727/1463/DC1
 Materials and Methods
 Figs. S1 to S5
 References

14 December 2004; accepted 23 March 2005
 10.1126/science.1108661